DALTON
FULL PAPER

Mutual effects on the spectroscopic and electrochemical properties of μ_3-oxo-trinuclear ruthenium complexes modified with a bridged [Ru(2,2′-bipy)$_2$(CN)] moiety †

Sofia Nikolaou and Henrique E. Toma *

Instituto de Química, Universidade de São Paulo, Caixa Postal 26077, Brazil.
E-mail: henetoma@iq.usp.br

Received 1st August 2001, Accepted 21st November 2001
First published as an Advance Article on the web 11th January 2002

The asymmetric dimers [$Ru_3O(CH_3COO)_6(py)_2$(B)Ru(2,2′-bipy)$_2$(L)](PF$_6$)$_2$, where B = 4,4′-bipy or bpa (1,2-*bis*(4-pyridyl)ethane) and L = Cl^- or CN^-, have been characterised based on spectroscopic and electrochemical techniques and both the influence of the CN^- coordination and of the bridging ligand have been studied. In the dimer where the bridging ligand is the π-conjugated 4,4′-bipy, the coordination of the cyanide ligand to the [Ru(2,2′-bipy)$_2$] moiety shifts to more positive values all the $E_{1/2}$ associated with the [Ru_3O] core. The influence of the [$Ru_3O(CH_3COO)_6(py)_2$] fragment on the spectroscopic properties of [Ru(2,2′-bipy)$_2$] has been probed by photophysical assays; at room temperature, no luminescence is detectable for the dimer where B = 4,4′-bipy, whereas the complex where B = bpa shows luminescence with low values of ϕ compared to the precursors [Ru(2,2′-bipy)$_2$(B)(CN)]PF$_6$. At 77 K both dimers show weak luminescence. Based on $\Delta G°$ values it is proposed that the main quenching pathway operates through an electron transfer mechanism.

Introduction

Trinuclear ruthenium complexes have been of great interest during the last decades, due to their remarkable electronic and electrochemical properties. These arise from the strong coupling of the three metal ions through the μ-oxo and carboxylate bridges.[1] These interactions are responsible for the rich electrochemical behaviour of these complexes, making them appropriate for the design of tunable multielectron redox catalysts.[2]

More recently, researchers have been concerned about using these trinuclear ruthenium complexes to assemble supramolecular structures[3–5] and to study intramolecular electron transfer reactions in symmetric dimers.[6] In this sense, the binding of those species to ruthenium polypyridine complexes, simulating [Ru(2,2′-bipy)$_3$]$^{+2}$,[7–10] would provide interesting prototypes to study photoinduced energy or electron transfer reactions.

The present study is focused on the asymmetric dimers shown in Fig. 1; the aim of the work is to assemble and compare the photophysical and electrochemical properties of two polynuclear complexes exhibiting different degrees of communication through the bridging ligands.

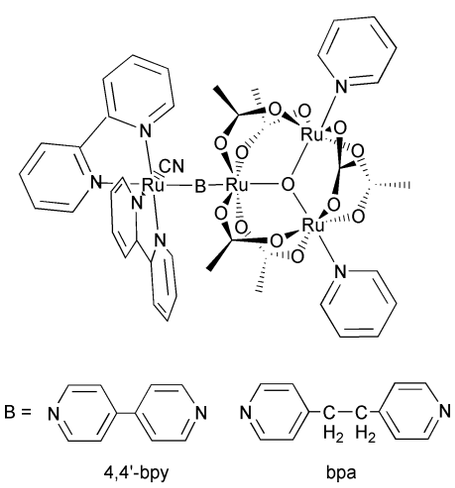

Fig. 1 Schematic structure of the asymmetric dimers [$Ru_3O(CH_3COO)_6(py)_2$(B)Ru(2,2′-bipy)$_2$(CN)](PF$_6$)$_2$.

Experimental

The starting asymmetric trinuclear complex [$Ru_3O(CH_3COO)_6(py)_2(CH_3OH)$]PF$_6$, as well as the precursors [Ru(2,2′-bipy)$_2$(B)(Cl)]PF$_6$ (B = 4,4′-bipy or bpa) have been synthesised as previously reported.[11,12]

Syntheses

[Ru(2,2′-bipy)$_2$(4,4′-bipy)(CN)]PF$_6$·CH$_2$Cl$_2$. [Ru(2,2′-bipy)$_2$(4,4′-bipy)(Cl)]PF$_6$ (790 mg, 1 mmol) was dissolved in a mixture of H_2O (35 cm^3) and C_2H_5OH (15 cm^3). After adding NaCN (73 mg, 1.5 mmol), the solution was allowed to react under reflux for 8 h, in the presence of a $N_{2(g)}$ atmosphere and light protected; the resulting material was left to rest overnight. Evaporation of C_2H_5OH led to the precipitation of a bright orange solid which was collected on a filter, dissolved in CH_3CN and purified by chromatography using a neutral alumina column. The main fraction was eluted with the same solvent and evaporated to dryness. The residue was dissolved in a minimum volume of CH_2Cl_2 and filtered onto stirring diethyl ether, yielding an orange solid which was dried under vacuum (363 mg, 44%). Found: C, 45.1; H, 3.2; N, 12.0. [Ru($C_{10}H_8N_2$)$_3$(CN)]PF$_6$·CH_2Cl_2 requires C, 46.5; H, 3.2; N, 11.9%. IR (KBr pellet): ν_{max}/cm^{-1} (CN) 2069 cm^{-1}.

[Ru(2,2′-bipy)$_2$(bpa)(CN)]PF$_6$·2CH$_2$Cl$_2$. This compound was synthesised as described above except a mixture of 8% C_2H_5OH : CH_3CN was used to elute the product from the chromatographic column (384 mg, 40%). Found: C, 45.8; H, 3.6; N, 10.2. [Ru($C_{10}H_8N_2$)$_2$($C_{12}H_{12}N_2$)(CN)]PF$_6$·2CH_2Cl_2 requires C, 44.8; H, 3.4; N, 10.4%. IR (KBr pellet): ν_{max}/cm^{-1} (CN) 2070 cm^{-1}.

† Electronic supplementary information (ESI) available: chemical shift values of the bpa dimer. See http://www.rsc.org/suppdata/dt/b1/b106973j/

 DOI: 10.1039/b106973j

$[Ru_3O(CH_3COO)_6(py)_2(4,4'\text{-bipy})Ru(2,2'\text{-bipy})_2(CN)](PF_6)_2\cdot CH_2Cl_2$. $[Ru(2,2'\text{-bipy})_2(4,4'\text{-bipy})(CN)]PF_6$ (300 mg, 0.364 mmol) was dissolved in CH_2Cl_2 (20 cm^{-3}) and allowed to react with $[Ru_3O(CH_3COO)_6(py)_2(CH_3OH)]PF_6$ (367 mg, 0.364 mmol) for 48 h, at room temperature and light protected. The solution was filtered, and the liquid was treated with diethyl ether, yielding a dark green solid. This material was collected on a filter, dissolved in CH_2Cl_2 and purified by chromatography using a neutral alumina column. The product was eluted with a mixture of 50% CH_3CN : CH_2Cl_2 and evaporated to dryness. After dissolving in a minimum volume of CH_2Cl_2, the solution was filtered onto stirring diethyl ether, yielding a green solid, which was dried under vacuum (53.2 mg, 8%). Found: C, 35.6; H, 2.9; N, 7.4. $[Ru_3O(CH_3COO)_6(C_5H_5N)_2Ru(C_{10}H_8N_2)_3(CN)](PF_6)_2\cdot CH_2Cl_2$ requires C, 35.9; H, 3.0; N, 7.0%. IR (KBr pellet): ν_{max}/cm^{-1} (CN) 2076 cm^{-1}.

$[Ru_3O(CH_3COO)_6(py)_2(bpa)Ru(2,2'\text{-bipy})_2(CN)](PF_6)_2\cdot 2CH_2Cl_2$. This compound was synthesised as described above except by the use of a mixture of 20% CH_3CN : CH_2Cl_2 to elute the product from the chromatographic column (40 mg, 8.7%). Found: C, 35.5; H, 3.2; N, 6.7. $[Ru_3O(CH_3COO)_6(C_5H_5N)_2(C_{12}H_{12}N_2)Ru(C_{10}H_8N_2)_2(CN)](PF_6)_2\cdot 2CH_2Cl_2$ requires C, 35.8; H, 3.2; N, 6.6%. IR (KBr pellet): ν_{max}/cm^{-1} (CN) 2077 cm^{-1}.

$[Ru_3O(CH_3COO)_6(py)_2(bpa)Ru(2,2'\text{-bipy})_2(Cl)](PF_6)_2$. $[Ru(2,2'\text{-bipy})_2(bpa)(Cl)]PF_6\cdot 2H_2O$ (122 mg, 0.149 mmol) was dissolved in CH_2Cl_2 (25 cm^3) and allowed to react with $[Ru_3O(CH_3COO)_6(py)_2(CH_3OH)]PF_6$ (150 mg, 0.149 mmol) for 48 h, at room temperature. The solution was filtered and the liquid was treated with diethyl ether, yielding a dark solid. This material was collected on a filter, dissolved in CH_2Cl_2 and purified by chromatography using a neutral alumina column. The product was eluted with a mixture of 20% CH_3CN : CH_2Cl_2 and evaporated to dryness. After dissolving in a minimum volume of CH_2Cl_2, the solution was filtered onto stirring diethyl ether, yielding a dark solid, which was dried under vacuum (39 mg, 15%). Found: C, 36.3; H, 3.2; N, 6.4. $[Ru_3O(CH_3COO)_6(C_5H_5N)_2(C_{12}H_{12}N_2)Ru(C_{10}H_8N_2)_2(Cl)](PF_6)_2$ requires C, 36.9; H, 3.2; N, 6.4%.

Measurements

One-dimensional ^1H NMR spectra and two dimensional COSY spectra were recorded on a Varian 300MHz spectrometer, model INOVA 1 and on a Brucker DRX 500 MHz spectrometer respectively, both data collected from 10^{-2} mol dm^{-3} CD_3CN solutions at room temperature. UV-visible spectra were recorded on a Hewlett Packard model 8453 diode array spectrophotometer from 10^{-5} mol dm^{-3} solutions. The infra-red spectra were obtained on a FTIR SHIMADZU spectrometer, model 8300, on a range 4000–400 cm^{-1}, with resolution of 4 cm^{-1}.

Cyclic voltammetry was carried out with a Princeton Applied Research model 283 potentiostat. A platinum disc electrode was employed for the measurements, using the conventional Luggin capillary arrangement with an $Ag/AgNO_3$ (0.010 mol dm^{-3}) reference electrode in CH_3CN containing 0.100 mol dm^{-3} tetraethylammonium perchlorate (TEAP). A platinum wire was used as the auxiliary electrode. All the $E_{1/2}$ values presented here were converted to SHE by summing 0.503 V to the observed values. A three electrode system was used for the spectroelectrochemical measurements, arranged in a rectangular quartz cell of 0.025 cm internal optical path length. A gold minigrid was used as transparent working electrode, in the presence of the above mentioned auxiliary and reference electrodes.

Steady-state emission and excitation spectra were recorded on a LS-100 Photon Technology International Inc. spectrophotometer. At room temperature a rectangular, four faced quartz cuvette was used for the mononuclear complexes and, in order to minimise reabsortion in the case of dimers, a triangular quartz cuvette was used. At 77 K a quartz tube of approximately 3 mm of diameter was used. Nanosecond emission decay measurements were obtained on a time-resolved LP900SI Edinburgh. Analytical Instruments spectrophotometer, constituted of a Nd-YAG (SureliteII-10) laser and a xenon lamp as the analytical beam. All the measurements were carried out from approximately 10^{-5} mol dm^{-3} solutions in different solvents.

The quantum yields were calculated from degassed CH_3CN solutions, using the known values of ϕ_s for $[Ru(2,2'\text{-bipy})_3]^{+2}$ at room temperature ($\phi_s = 0.086$) and from ethanol glass at 77 K ($\phi_s = 0.376$)[7] and the integrated areas under the emission curve corrected by the relative absorbance at the excitation wavelength.[13]

Results and discussion

NMR Spectroscopy

The COSY spectrum of the bpa dimer is presented in Fig. 2.

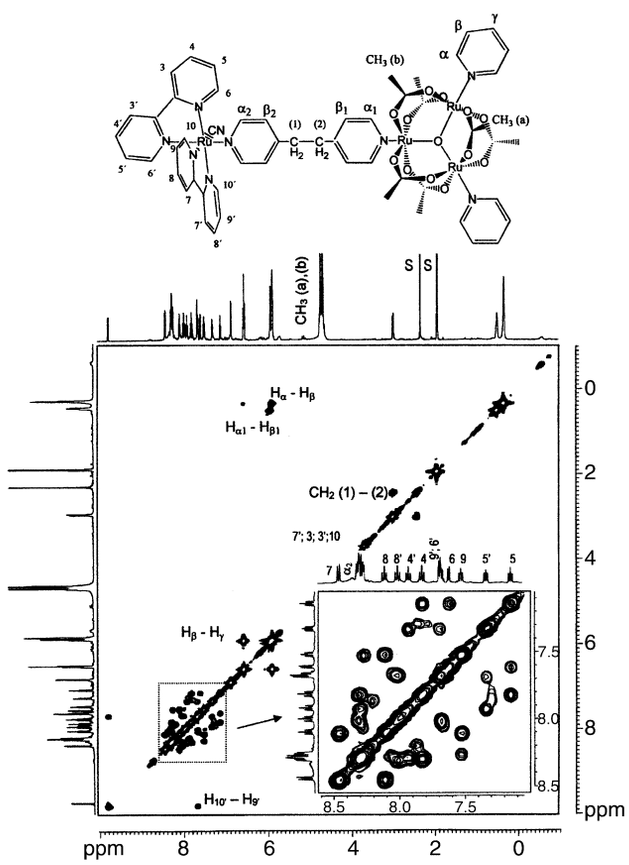

Fig. 2 COSY plots for $[Ru_3O(CH_3COO)_6(py)_2(bpa)Ru(2,2'\text{-bipy})_2(CN)](PF_6)_2$ in 10^{-2} mol dm^{-3} CD_3CN solution (S = solvent peak).

Although a suitable crystalline material for X-ray studies has not been obtained up to the present time, the two dimensional COSY NMR spectra of that dimer is completely consistent with the proposed structure (a detailed discussion on the structural characterisation based on NMR techniques of a mixed trinuclear complex–ruthenium polypyridine dimer has been presented elsewhere,[14] as well as the full assignment of the $[Ru_3O(CH_3COO)_6(py)_2(4,4'\text{-bipy})Ru(2,2'\text{-bipy})_2(Cl)](PF_6)_2$ analogue).[11]

The spectrum is rather complicated due to the large number of signals. The non-magnetic equivalence of all pyridinic rings (except the two py rings), accounts for the signals splitting in the aromatic region of the spectrum. The assignment was

guided by the observed correlations and comparison with literature results.[11,14–16]

The signals observed for the [Ru(2,2′-bipy)$_2$] unit follow the same trends observed for the [Ru(2,2′-bipy)$_3$]$^{+2}$ and [Ru(2,2′-bipy)$_2$(CN)$_2$] analogues, due to *ring current* effects of the bipy and bpa ligands and deshielding effect caused by the induced electron circulation in the CN triple bond.[15,16] It is worth mentioning the larger splitting between protons attached to the same positions of bipy rings, *e.g.* H_5 and $H_{5'}$, when compared to the complexes [Ru$_3$O(CH$_3$COO)$_6$(py)$_2$(4,4′-bipy)Ru(2,2′-bipy)$_2$(Cl)](PF$_6$)$_2$[11] and [Ru$_3$O(CH$_3$COO)$_6$(py)$_2$(tmbipy)Ru(2,2′-bipy)$_2$(Cl)](PF$_6$)$_2$ (tmbipy = trimethylenedipyridine).[14] This fact also reflects the significant disturbance of the electron density on the [Ru(2,2′-bipy)$_2$] unit caused by the cyanide coordination.

In the case of the [Ru$_3$O(CH$_3$COO)$_6$(py)$_2$] moiety, the observed pattern is dictated by the paramagnetic anisotropy of the [Ru$_3$O] core, which contains one unpaired electron. The α-protons of the pyridinic rings attached directly to the paramagnetic centre exhibit large shifts to higher field in relation to the free ligands. This effect decreases with distance, being less pronounced for β and γ-protons. On the other hand the acetate protons, which are split due to differences in chemical environment, are shifted in the opposite direction to those of pyridines. This pattern of chemical shifts can only be explained by taking into account both dipolar and contact mechanism for the paramagnetic interactions in the molecule.

IR Vibrational spectroscopy

The IR peaks corresponding to the ν(CN) vibration of the mononuclear precursors [Ru(2,2′-bipy)$_2$(B)(CN)]PF$_6$ and of the dimers are shown in Fig. 3. From the profiles observed it is

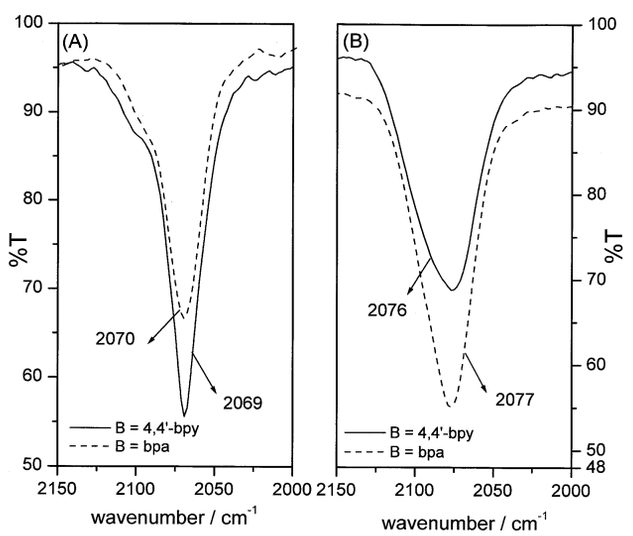

Fig. 3 Infrared spectra of (A) [Ru(2,2′-bipy)$_2$(B)(CN)]PF$_6$ and (B) [Ru$_3$O(CH$_3$COO)$_6$(py)$_2$(B)Ru(2,2′-bipy)$_2$(CN)](PF$_6$)$_2$ in the CN stretching region obtained from KBr pellets.

clear that a cyanide group is coordinated to the [Ru(2,2′-bipy)$_2$] moiety.[17–19] Also, the stretching frequencies have typical values of monodentate CN groups coordinated to a ruthenium centre,[18] thus excluding the possibility that the cyanide is a bridging ligand in the dimers.

Absorption spectra and solvent effect

Fig. 4 shows the electronic spectra of the mixed species. The main features observed may be easily interpreted by comparison with the reported data for [Ru(2,2′-bipy)$_2$(CN)$_2$][17,20] and [Ru$_3$O(CH$_3$COO)$_6$(py)$_2$(B)]PF$_6$ (B = bridging ligand).[12] The intense bands in the ultra-violet region can be assigned to the pyridinic ligands π ⟶ π* transitions; in the visible region the MLCT bands of the [Ru(2,2′-bipy)$_2$] unit can be observed,

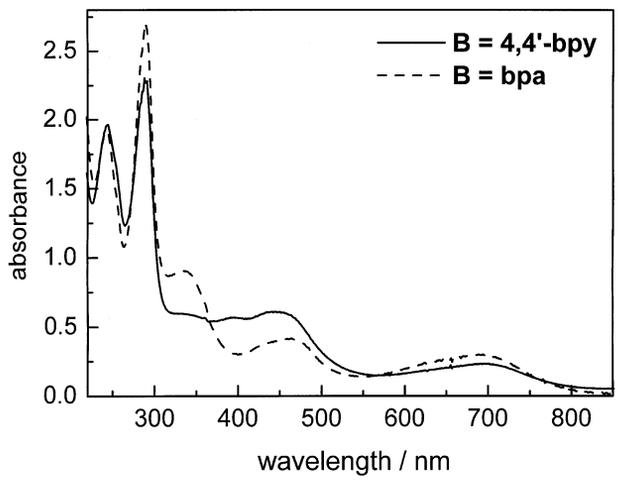

Fig. 4 Absorption spectra of the dimer [Ru$_3$O(CH$_3$COO)$_6$(py)$_2$(B)Ru(2,2′-bipy)$_2$(CN)](PF$_6$)$_2$ in acetonitrile solutions.

as confirmed by their solvent dependence and by the spectroelectrochemical measurements (see below). Finally, the near infra-red broad band is consistent with the typical IC (intracluster) transitions within an energy level manifold, generated by the combination of the ruthenium and central oxygen orbitals in the [Ru$_3$O(CH$_3$COO)$_6$] fragment.[1,12] The cluster-to-ligand charge transfer (CLCT) bands, which involve a molecular orbital of the [Ru$_3$O] center and the ligand π* level, are hidden under the MLCT bands of the [Ru(2,2′-bipy)$_2$] chromophore.

According to the data summarised in Table 1, the cyanide coordination promotes a blue shift of the MLCT bands in the [Ru(2,2′-bipy)$_2$] fragment; the π-backbonding between the CN ligand and the metal centre, which stabilise the d_π levels, accounts for this effect. On the other hand, the dimer MLCT bands exhibit a slight shift to higher energy if compared to the values observed for the [Ru(2,2′-bipy)$_2$(B)(CN)]PF$_6$ complexes, indicating that the trinuclear complex might be acting as a withdrawing group in the mixed species. Nevertheless, this effect is less pronounced than the removal of electronic density by the CN ligand.

To assign unequivocally the bands at 397 nm and 445 nm of the [Ru$_3$O(CH$_3$COO)$_6$(py)$_2$(4,4′-bipy)Ru(2,2′-bipy)$_2$(CN)](PF$_6$)$_2$ complex, we have carried out a qualitative titration with diluted H_2SO_4 of that complex and of the precursor [Ru(2,2′-bipy)$_2$(4,4′-bipy)(CN)]PF$_6$ (Fig. 5).

In the case of [Ru(2,2′-bipy)$_2$(4,4′-bipy)(CN)]PF$_6$ we expected two distinct protonation processes: one for the cyanide and other for the 4,4′-bipy ligand; the bridging ligand in its turn can not be protonated in the dimer. The first process observed for [Ru(2,2′-bipy)$_2$(4,4′-bipy)(CN)]PF$_6$ was assigned to the protonation of the bridging ligand 4,4′-bipy. For both complexes we observed a intensity decay of the MLCT bands around 450 nm and a shift towards 400 nm. This process, common for both mononuclear and mixed species, was assigned to the protonation of the CN ligand. It is important to note that the charge transfer band at 397 nm in the dimer is not affected, being thus consistent with a CLCT band.

Fig. 6 illustrates the dependence of the MLCT band energy on the solvent parameter acceptor number.[20,21] The values of AN were those found in reference 21(*b*). The observed correlations demonstrate that, as previously reported for a number of related systems,[20,21*a*] the interaction between complex and solvent molecules has a donor–acceptor nature and it takes place mainly through the lone electron pair in the CN ligand. The observed blue-shift can be rationalised in terms of an electron density decrease on the metal centre, since the cyanide ligand is involved in a donor interaction with solvent molecules. The smaller effect found in the dimers when compared to

Table 1 Absorption spectral data for the dimers and correlated species

Complex	$\lambda_{máx}$/nm (log ε/mol^{-1} dm^3 cm^{-1})			
	MLCT	CLCT	MLCT	IC
$[Ru_3O(CH_3COO)_6(py)_2(4,4'\text{-bipy})Ru(2,2'\text{-bipy})_2(CN)](PF_6)_2$	330 (sh)	397 (4.06)	445 (4.11)	692 (3.73)
$[Ru_3O(CH_3COO)_6(py)_2(4,4'\text{-bipy})Ru(2,2'\text{-bipy})_2(Cl)](PF_6)_2$ [a]	396 (4.11)	343 (4.12)	489 (4.13)	692 (3.77)
$[Ru(2,2'\text{-bipy})_2(4,4'\text{-bipy})(CN)]PF_6$	361 (4.03)		451 (4.10)	
$[Ru_3O(CH_3COO)_6(py)_2(bpa)Ru(2,2'\text{-bipy})_2(CN)](PF_6)_2$	336 (4.32)		462 (3.97)	689 (3.82)
$[Ru_3O(CH_3COO)_6(py)_2(bpa)Ru(2,2'\text{-bipy})_2(Cl)](PF_6)_2$	345 (4.25)		502 (3.98)	692 (3.77)
$[Ru(2,2'\text{-bipy})_2(bpa)(CN)]PF_6$	342 (4.08)		467 (3.94)	

[a] Data from ref. 11.

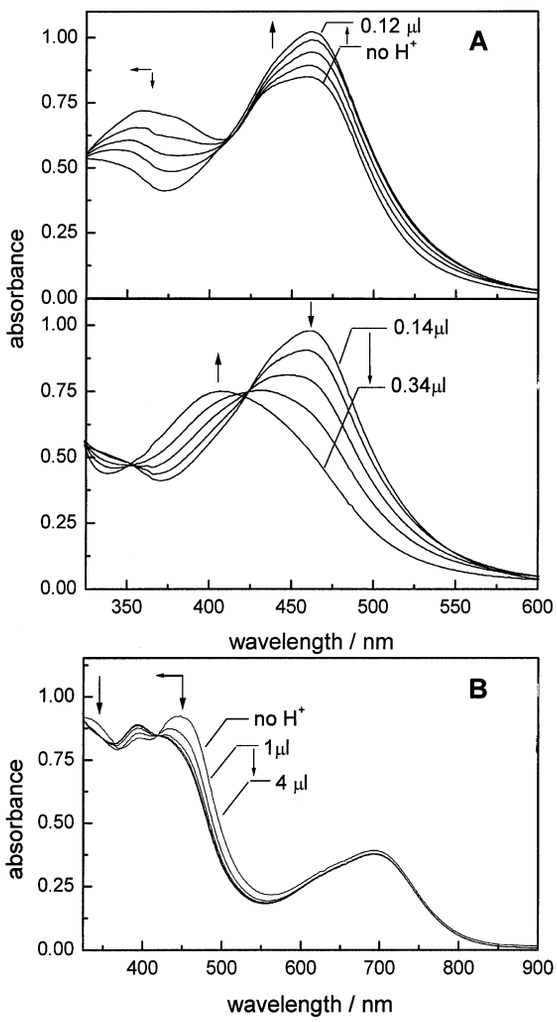

Fig. 5 Titration of (A) the mononuclear complex $[Ru(2,2'\text{-bipy})_2(4,4'\text{-bipy})(CN)]PF_6$ and (B) the mixed dimer $[Ru_3O(CH_3COO)_6(py)_2(4,4'\text{-bipy})Ru(2,2'\text{-bipy})_2(CN)](PF_6)_2$ in CH_3CN solutions with aqueous H_2SO_4 (0.01 mol dm^{-3} and 0.1 mol dm^{-3} respectively).

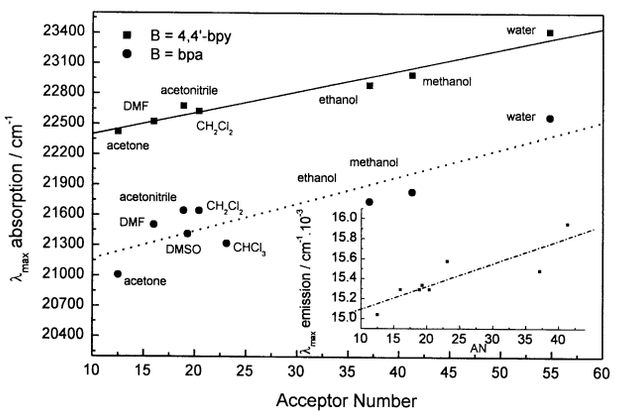

Fig. 6 MLCT absorption energy of the $[Ru_3O(CH_3COO)_6(py)_2(B)Ru(2,2'\text{-bipy})_2(CN)](PF_6)_2$ dimers *vs.* acceptor number (■) B = 4,4′-bipy and (●) B = bpa. The inset shows the dependence of the bpa dimer emission band at room temperature.

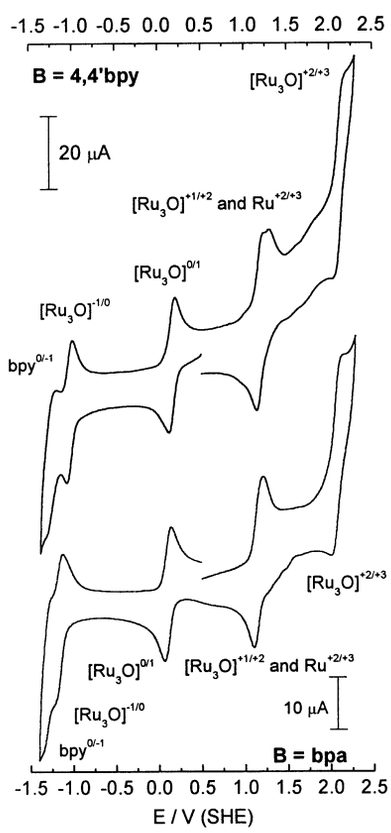

Fig. 7 Cyclic voltammograms of $[Ru_3O(CH_3COO)_6(py)_2(B)Ru(2,2'\text{-bipy})_2(CN)](PF_6)_2$ in 10^{-3} mol dm^{-3} acetonitrile solutions, 0.1 mol dm^{-3} TEAP, room temperature, scan rate: 50 mV s^{-1}.

complexes like $[M(2,2'\text{-bipy})_n(CN)_{m-n}]$ (M = Ru[20] or Fe[21a]), reflects the presence of only one CN ligand in the molecule. Also in Fig. 6 one can see that the emission band of the bpa dimer follow the same trend as the absorption band, showing that both absorption and emission have the same MLCT orbital nature.

Electrochemical measurements

The voltammogram profile is similar to one of a ruthenium trinuclear complex bounded to N-heterocyclic ligands (Fig. 7) and it basically shows five sets of waves associated with four successive monoelectronic redox processes of the $[Ru_3O]$ core and with the reduction of the peripheral 2,2′-bipy ligand. For B = 4,4′-bipy, one can see the splitting in the anodic peak assigned to the $[Ru_3O]^{+1/+2}$ and $Ru^{+2/+3}$ pairs, which is not observed for B = bpa. However, based on the spectroelectrochemical measurements (see below), we could unequivocally

Table 2 Electrochemical data for $[Ru_3O(CH_3COO)_6(py)_2(B)Ru(2,2'\text{-bipy})_2(CN)]^{+2}$ and for the related $[Ru_3O(CH_3COO)_6(py)_2(B)Ru(2,2'\text{-bipy})_2(Cl)]^{+2}$ complexes in parentheses[a] (the redox processes of $[Ru_3O(CH_3COO)_6(py)_2]$ are represented by $[Ru_3O]^n$)

	2,2′-bipy$^{0/-1}$	$[Ru_3O]^{-1/0}$	$[Ru_3O]^{0/+1}$	$[Ru_3O]^{+1/+2}$	$Ru^{+2/+3}$	$[Ru_3O]^{+2/+3}$
B = 4,4′-bipy	−1.24	−1.03 (−1.06)	0.16 (0.15)	1.19 (1.17)	1.30 (0.98)	2.12 (2.09)
B = bpa	−1.29	−1.15 (−1.13)	0.11 (0.13)	1.16 (1.17)	1.16 (0.95)	2.08 (2.10)
$[Ru(2,2'\text{-bipy})_2(4,4'\text{-bipy})(CN)]PF_6$	−1.24				1.28	
$[Ru(2,2'\text{-bipy})_2(bpa)(CN)]PF_6$	−1.28				1.23	

[a] Data from reference 11 for $[Ru_3O(CH_3COO)_6(py)_2(4,4'\text{-bipy})Ru(2,2'\text{-bipy})_2(Cl)]^{+2}$.

assign the $[Ru_3O]^{+1/+2}$ and $Ru^{+2/+3}$ pairs in $[Ru_3O(CH_3COO)_6(py)_2(bpa)Ru(2,2'\text{-bipy})_2(CN)]^{+2}$, superimposed under the wave at 1.16 V.

Compared to the $[Ru_3O(CH_3COO)_6(py)_2(B)Ru(2,2'\text{-bipy})_2(Cl)]^{+2}$ complexes (see Table 2), there are $E_{1/2}$ shifts in all redox processes of the mixed species. The π-backbonding between the cyanide and the metal centre stabilise the d_π levels of $[Ru(2,2'\text{-bipy})_2]$, turning it more stable in the Ru^{+2} oxidation state. The fact that the $[Ru_3O]$ redox processes are also affected confirms the weak interaction between the fragments.

On the other hand, one can observe that in the mixed species, as in monomeric trinuclear complexes,[22] the $[Ru_3O]$ core is sensitive to the coordinated N-heterocyclic ligands; actually for B = bpa the $[Ru_3O]$ redox couples are negatively shifted in comparison to the 4,4′-bipy dimer reflecting the σ-donor character of the former ligand.

In Fig. 8 one can see the absorption spectra of the mixed

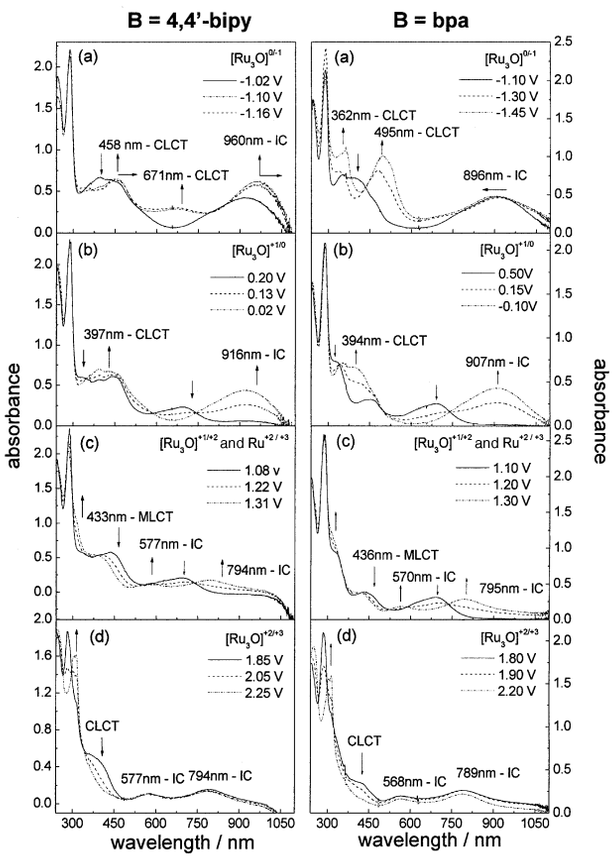

Fig. 8 Spectroelectrochemical behaviour of the mixed trinuclear complexes $[Ru_3O(CH_3COO)_6(py)_2(B)Ru(2,2'\text{-bipy})_2(CN)](PF_6)_2$ in acetonitrile solutions.

complexes at several applied potentials. The first reduction process of the $[Ru_3O(CH_3COO)_6(py)_2]$ moiety (Fig. 8(b)), corresponds to the $Ru^{III}Ru^{III}Ru^{III}/Ru^{III}Ru^{III}Ru^{II}$ step, which involves a large IC band bathochromic shift from approximately 690 nm to 910 nm. The addition of one electron to the $[Ru_3O]$ core results in the overall destabilisation of its electronic levels, being responsible for the red shift of the IC band.[11,12] Moreover, the CLCT bands also suffer bathochromic shifts, causing the intensification observed in the range between 300 and 450 nm.

The $[Ru_3O(CH_3COO)_6(py)_2]$ moiety second reduction, shown in Fig. 8(a), corresponds to the $Ru^{III}Ru^{III}Ru^{II}/Ru^{III}Ru^{II}Ru^{II}$ process. Analogously to the preceding step, it is also accompanied by additional CLCT band red shifts, as a consequence of the larger destabilisation on the $[Ru_3O]$ core electronic levels. It is worth noting the appearance of a new band at 671 nm for the complex $[Ru_3O(CH_3COO)_6(py)_2(4,4'\text{-bipy})Ru(2,2'\text{-bipy})_2(CN)](PF_6)_2$, ascribed to the cluster ⟶ 4,4′-bipy charge-transfer band. The bathochromic shift in this CLCT band is consistent with a strong electronic coupling, as in the extended structures previously reported in the literature in which the 4,4′-bipy ligand acts as a bridge, connecting trinuclear ruthenium complexes units[4b] or the $[Ru(2,2'\text{-bipy})_2(Cl)]$ fragment.[11] For the third reduction process observed in the cyclic voltammetry, the spectroelectrochemical measurement was not reproducible because of the high limiting potential employed.

The first oxidative process is shown in Fig. 8(c). The splitting pattern followed by the IC band corresponds to the oxidation of the $[Ru_3O(CH_3COO)_6(py)_2]$ unit, from the formal $Ru^{III}Ru^{III}Ru^{III}$ state to the $Ru^{IV}Ru^{III}Ru^{III}$ state.[11,12] This splitting can be explained in terms of an unequal d_π level stabilisation due to the removal of one electron from the $[Ru_3O]$ core. Concomitantly, the oxidation of the Ru ion in the $[Ru(2,2'\text{-bipy})_2]$ moiety takes place, as deduced from the decay of the characteristic MLCT band around 430 nm, and from the shift of the 2,2′-bipy π ⟶ π* band to higher energy. This observation supports the assignment of the voltammetric wave at 1.16 V (for B = bpa) to both $[Ru_3O]^{+1/+2}$ and $Ru^{+2/+3}$ oxidation processes.

It is relevant to consider that the decay in the MLCT and the $[Ru_3O]$ oxidation evidences another CLCT band (shoulder between 400 nm and 450 nm), which decays when the potential range is scanned from about 1.80 V to 2.20 V (Fig. 8(d). This observation supports the assignment of the last redox couple as $Ru^{IV}Ru^{III}Ru^{III}/Ru^{IV}Ru^{IV}Ru^{III}$. Parallel to the CLCT decay, we observed the continuous shift to higher energy of the 2,2′-bipy π ⟶ π* band, showing once more that the oxidation processes of both $[Ru(2,2'\text{-bipy})_2]$ and $[Ru_3O(CH_3COO)_6(py)_2]$ moieties are coupled. Although it was possible to delineate the above conclusions, the results observed for the last oxidation might be disturbed due to the high limiting potential employed, especially in dealing with a gold electrode.[23]

Photophysical assays

The luminescence spectra of the precursor complexes $[Ru(2,2'\text{-bipy})_2(B)(CN)]PF_6$ exhibit strong bands with λ_{em} in the range 600–700 nm (Table 3), which were ascribed to the emission of the lowest triplet excited state, in parallel with the $[Ru(2,2'\text{-bipy})_3]^{+2}$ complex.[7] The respective excitation profile reproduces the absorption MLCT band, showing the efficient internal conversion and intersystem crossing involving the molecular excited states. The emission quantum yields are also shown in Table 3. The luminescence intensities are strongly dependent on the presence of dissolved oxygen in solution, presenting a reduction of about 40% for non degassed solutions.

Table 3 Photophysical data for the mononuclear complexes and for the dimers in different oxidation states (represented here by [Ru(2,2′-bipy)$_2$(B)[Ru$_3$O]) at room temperature (acetonitrile solutions) and at 77 K (ethanol glasses)

Complex	At room temperature			
	λ_{em}/nm	λ_{exc}/nm	ϕ_{em}	$\tau_{1/2}$/μs
[Ru(2,2′-bipy)$_2$(4,4′-bipy)(CN)]PF$_6$	695	455	0.063	0.12
[Ru(2,2′-bipy)$_2$(bpa)(CN)]PF$_6$	660	478	0.011	0.21
[Ru^{+2}(2,2′-bipy)$_2$](4,4′-bipy)[Ru$_3$O]$^{+1}$	[a]	455		
[Ru^{+2}(2,2′-bipy)$_2$](bpa)[Ru$_3$O]$^{+1}$	654	478	0.003 0.0026[b]	[d]
[Ru^{+2}(2,2′-bipy)$_2$](bpa)[Ru$_3$O]^{0} [c]			0.0018[b]	

	At 77 K				
	λ_{exc}/nm	ϕ_{em}	E_{0-0}/eV[e]	$\Delta G°_{oxi}$/eV[f]	$\Delta G°_{red}$/eV
[Ru^{+2}(2,2′-bipy)$_2$](4,4′-bipy)[Ru$_3$O]$^{+1}$	455	0.007	2.128	−0.99	
[Ru^{+2}(2,2′-bipy)$_2$](4,4′-bipy)[Ru$_3$O]^{0}	455	0.008	2.135		−0.74
[Ru^{+2}(2,2′-bipy)$_2$](bpa)[Ru$_3$O]$^{+1}$	478	0.028	2.143	−1.09	
[Ru^{+2}(2,2′-bipy)$_2$](bpa)[Ru$_3$O]^{0}	478	0.015	2.136		−0.74

[a] This dimer did not show emission at room temperature. [b] Data collected in ethanolic solution for comparison purposes. [c] N_2H_4(aq) was used as reduction agent. [d] No transient was detected in a time scale up to 5 ns. [e] E_{0-0} taken from the low-temperature emission spectra. [f] Calculated values of $\Delta G°$ for the excited state electron transfer reaction.

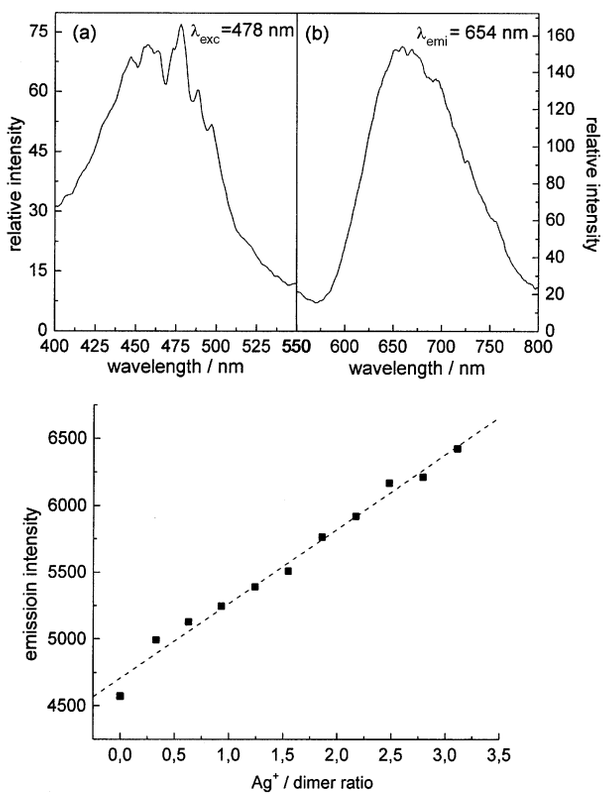

Fig. 9 Top: (a) Excitation and (b) emission spectra of [Ru$_3$O(CH$_3$COO)$_6$(py)$_2$(bpa)Ru(2,2′-bipy)$_2$(CN)](PF$_6$)$_2$ in 2 × 10^{-5} mol dm^{-3} acetonitrile degassed solution, at room temperature. Bottom: Titration of a 5 × 10^{-5} mol dm^{-3} dimer solution with a 4 × 10^{-3} mol dm^{-3} solution of AgNO$_3$, both in acetonitrile. The emission intensity was calculated from the area under the emission curve, corrected for dilution effects.

The dimers exhibited different behaviour. In the case of B = 4,4′-bipy we were not able to observe emission at room temperature, in contrast to the bpa dimer, which presents an emission profile typical of a [Ru(2,2′-bipy)$_n$] group (see Fig. 9), but with low values of ϕ_{em} as compared to the mononuclear precursors; also we could not detect a transient decay in a time scale up to 5 ns. These results led us to conclude that the [Ru$_3$O(CH$_3$COO)$_6$(py)$_2$] moiety quenches the luminescence of the [Ru(2,2′-bipy)$_2$(CN)] group through a fast mechanism, especially when the bridge connecting the chromophores is the π-conjugated 4,4′-bipy. For the bpa dimer, the quenching mechanism is less effective due to the electronic isolation of the units promoted by that ligand.

In order to obtain information about the excited-state behaviour in the bpa dimer we carried out a titration with a Ag$^+$ acetonitrile solution; the result is also shown in Fig. 9. Under the conditions employed, the main product formed in solution should be the cyano–Ag$^+$ mono-coordinated adduct (because of steric reasons we exclude the possibility that two dimer molecules are bridged through a CN–Ag–CN bond). Kinnaird and Whitten[24] have observed a similar pattern of increasing emission intensity for the mononuclear complex [Ru(2,2′-bipy)$_2$(CN)$_2$] upon Ag$^+$ addition, although in that case the intensity increase was accompanied by a blue shift of both absorption and emission bands, which is consistent with the sharing of the CN lone pair of electrons in the CN–metal bond. In the present case we did not observe such shifts; therefore it seemed reasonable to interpret the prominent emission intensity increase in terms of a k_{nr} decrease, either by decreasing internal conversion or by changing significantly the solvation interactions.

At 77 K both dimers show emission bands (Fig. 10), with an

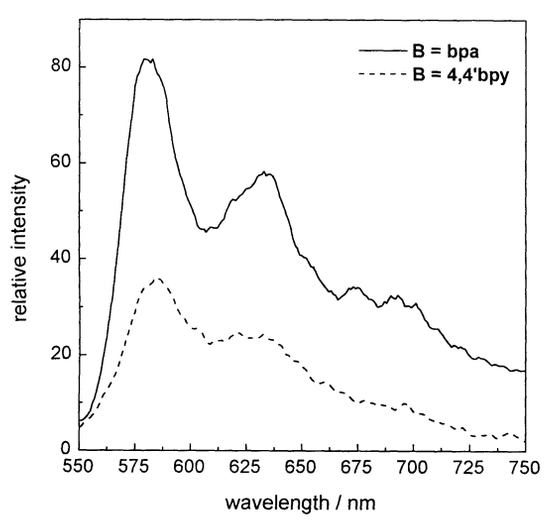

Fig. 10 Low temperature (77 K) emission spectra of [Ru$_3$O(CH$_3$COO)$_6$(py)$_2$(B)Ru(2,2′-bipy)$_2$(CN)](PF$_6$)$_2$ in ethanol glasses.

evident vibrational progression (of *ca.* 1000 cm^{-1} for B = 4,4′-bipy and *ca.* 1400 cm^{-1} for B = bpa), but still with low values of ϕ_{em} (see Table 3).

There are two possible intramolecular quenching mechanisms: energy or electron transfer. According to thermodynamics, energy transfer depends on the excited state energy, while electron transfer depends mainly on the excited state oxidation and reduction potentials.[8a,10,25,26]

Considering an electron transfer quenching, we have calculated the driving force for this reaction accordingly to Schemes 1 and 2: [10,25]

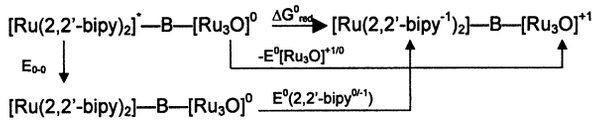

Scheme 1 $\Delta G°_{red} = -[E_{0\text{-}0} - E°[Ru_3O]^{+1/0} + E°(2,2'\text{-bipy}^{0/-1})]$ (reductive quenching).

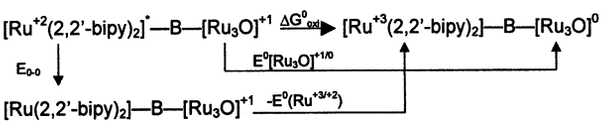

Scheme 2 $\Delta G°_{oxi} = -[E_{0\text{-}0} - E°(Ru^{+3/+2}) + E°[Ru_3O]^{+1/0}]$ (oxidative quenching).

From the calculated values of $\Delta G°$ (Table 3), the oxidative quenching mechanism is more favourable, and this reaction would occur in the oxidised dimers. The quantum yields exhibit an opposite trend from that expected based on thermodynamics, once the emission is more intense in the case where the quenching is favourable. This fact led us to consider the energy transfer contribution to the quenching in the reduced dimers.

The requirement of overlap between the donor emission and the acceptor absorption bands in the Foster type mechanism of energy transfer[26] is fulfilled by the dimers under question. However, the spin restriction imposed by this model would prevent this mechanism from operating in the mixed complexes. On the other hand, the ground and excited state of the reduced $[Ru_3O(CH_3COO)_6]$ fragment are a singlet and a triplet, respectively. This meets the spin conservation of the dimer foreseen in the exchange energy transfer mechanism (Dexter type).[10a] On this basis we can conclude that, at least for the reduced bpa dimer, the Dexter energy transfer contributes to the emission quenching of the $[Ru(2,2'\text{-bipy})_2]$ chromophore by the $[Ru_3O(CH_3COO)_6]$ acceptor, which accounts for the lower values of ϕ_{em} in ethanolic media, both at room and low (77K) temperatures (Table 3).

It is worth mentioning that, for the 4,4′bipy dimer the ϕ_{em} values are almost unchanged by the chemical reduction of the dimer. It shows that the bridge size and its π-conjugating nature strongly favour the quenching, despite the mechanism.

In previous studies on bimolecular quenching involving $[Ru(2,2'\text{-bipy})_3]^{+2}$ and trinuclear ruthenium complexes it was concluded that luminescence quenching occurs as a function of photoinduced energy transfer.[27] On the other hand, it was shown that in mixed porphyrin–trinuclear ruthenium complexes systems the quenching of the Zn porphyrin fluorescence is accomplished by a photoinduced electron transfer in a femtosecond time scale.[28]

Under the conditions employed in this work we can not definitely conclude which of the above mechanisms prevail in the dimers. Yet, we demonstrated that the $[Ru_3O(CH_3COO)_6(py)_2]$ group is a good quencher at room temperature, acting very efficiently when the bridge connecting donor and acceptor allows π-conjugation, and still operating when the bridge isolates the groups.

Conclusion

In this work we have reported the synthesis and characterisation of the mixed dimers $[Ru_3O(CH_3COO)_6(py)_2(B)Ru(2,2'\text{-bipy})_2(CN)](PF_6)_2$. In comparison to the non luminescent $[Ru_3O(CH_3COO)_6(py)_2(B)Ru(2,2'\text{-bipy})_2(Cl)](PF_6)_2$ complexes, the electronic and electrochemical properties of the mixed dimers reflect the coordination of the π-acceptor CN ligand in the peripheral $[Ru(2,2'\text{-bipy})_2]$ group. The most relevant feature observed through the electrochemical measurements is the electronic communication of the chromophores, especially for the dimer where B = 4,4′-bipy, as reflected in the coupling of the redox processes of both $[Ru(2,2'\text{-bipy})_2]$ and $[Ru_3O(CH_3COO)_6(py)_2]$ moieties. This mutual interaction is confirmed by the intramolecular luminescence quenching observed for the dimers.

All the results observed are consistent with a weakly interacting mixed complex in which the electronic interaction between donor and acceptor is modulated by the bridging ligand, as a function of its size and π-conjugating nature. Consequently, these dimers can be seen as prototypes of electronically coupled polymetallic systems and also as protagonists of fast photoinduced electron and energy transfer reactions.

Acknowledgements

The financial support from the Brazilian Agencies FAPESP and CNPq is gratefully acknowledged.

References

1 H. E. Toma, K. Araki, A. D. P. Alexiou, S. Nikolaou and S. Dovidauskas, *Coord. Chem. Rev.*, 2001, **219–221**, 187.
2 (*a*) H. E. Toma and A. D. P. Alexiou, *J. Chem. Res. (S)*, 1993, 464; (*b*) selected references: S. B. Marr, R. O. Carvel, D. T. Richens, H. Lee, M. Lane and P. Stavropoulos, *Inorg. Chem.*, 2000, **39**, 4630; (*c*) S. Cosnier, A. Deronzier and A. Llobet, *J. Electroanal. Chem.*, 1990, **280**, 213; (*d*) C. P. Nicolaides and N. J. Coville, *J. Mol. Catal.*, 1984, **21**, 375; (*e*) S. Ito, K. Aihara and M. Matsumoto, *Tetrahedron Lett.*, 1983, **24**, 5249; (*f*) T. Szymanska-Buzar and J. J. Ziólkowski, *J. Mol. Catal.*, 1981, **11**, 371; (*g*) S. A. Fouda, B. C. Y. Hui and G. L. Rempel, *Inorg. Chem.*, 1978, **17**, 3213.
3 S. Nikolaou and H. E. Toma, *J. Chem. Res. (S)*, 2000, 326.
4 (*a*) H. E. Toma and A. D. P. Alexiou, *J. Braz. Chem. Soc.*, 1995, **6**, 267; (*b*) H. E. Toma and A. D. P. Alexiou, *J. Chem. Res. (S)*, 1995, 134.
5 (*a*) K. Araki, S. Dovidauskas, H. Winnischofer, A. D. P. Alexiou and H. E. Toma, *J. Electroanal. Chem.*, 2001, **498**, 152; (*b*) S. Dovidauskas, K. Araki and H. E. Toma, *J. Porphyrins Phthalocyanines*, 2000, **4**, 727; (*c*) S. Dovidauskas, H. E. Toma, K. Araki, H. C. Sacco and Y. Iamamoto, *Inorg. Chim. Acta*, 2000, **305**, 206; (*d*) H. E. Toma, K. Araki and E. O. Silva, *Monatsh. Chem.*, 1998, **129**, 975.
6 (*a*) T. Yamaguchi, N. Imai, T. Ito and C. P. Kubbiak, *Bull. Chem. Soc. Jpn.*, 2000, **73**, 1205; (*b*) I. S. Zavarine, C. P. Kubbiak, T. Yamaguchi, K. Ota, T. Matsui and T. Ito, *Inorg. Chem.*, 2000, **39**, 2696; (*c*) T. Ito, T. Hamaguchi, H. Nagino, T. Yamaguchi, H. Kido, I. S. Zavarine, T. Richmond, J. Washington and C. P. Kubbiak, *J. Am. Chem. Soc.*, 1999, **121**, 4625; (*d*) T. Ito, T. Hamaguchi, H. Nagino, T. Yamaguchi, J. Washington and C. P. Kubbiak, *Science*, 1997, **227**, 660.
7 A. Juris, V. Balzani, F. Barigelletti, S. Campagna, P. Belser and A. von Zelewsky, *Coord. Chem. Rev.*, 1988, **84**, 85.
8 (*a*) V. Balzani, A. Juris, M. Venturi, S. Campagna and S. Serroni, *Chem. Rev.*, 1996, **96**, 759; (*b*) L. de Cola and P. Belser, *Coord. Chem. Rev.*, 1998, **177**, 301.
9 (*a*) C. A. Bignozzi, R. Argazzi, O. Bertolini, F. Scandola and A. Harriman, *New J. Chem.*, 1996, **20**, 731; (*b*) F. Scandola, R. Argazzi, C. A. Bignozzi and M. T. Indelli, *J. Photochem. Photobiol., A*, 1994, **82**, 191; (*c*) F. Scandola, R. Argazzi, C. A. Bignozzi, C. Chiorboli, M. T. Indelli and M. A. Rampi, *Coord. Chem. Rev.*, 1993, **125**, 283.
10 (*a*) V. Balzani and F. Scandola, in *Supramolecular Photochemistry*, Ellis Horwood, Chichester, 1991; (*b*) R. Bergonzi, L. Fabbrizzi, M. Licchelli and C. Mangano, *Coord. Chem. Rev.*, 1998, **170**, 31.
11 S. Nikolaou and H. E. Toma, *Polyhedron*, 2001, **20**, 253.

12 J. A. Baumann, D. J. Salmon, S. T. Wilson, T. J. Meyer and W. E. Hatifield, *Inorg. Chem.*, 1978, **17**, 3342.
13 S. F. McClanahan, R. F. Dallinger, F. J. Holler and J. R. Kincard, *J. Am. Chem. Soc.*, 1985, **107**, 4853.
14 S. Nikolaou, M. Uemi and H. E. Toma, *Spectrosc. Lett.*, 2001, **34**, 267.
15 E. C. Constable and J. Lewis, *Inorg. Chim. Acta*, 1983, **70**, 251.
16 (*a*) M. Marayama, H. Matzuzawa and Y. Kaizu, *Inorg. Chim. Acta*, 1995, **237**, 159; (*b*) J. M. Malin, C. F. Schmidt and H. E. Toma, *Inorg. Chem.*, 1975, **14**, 2924.
17 C. A. Bignozzi and F. Scandola, *Inorg. Chem.*, 1984, **23**, 1540.
18 A. A. Schilt, *Inorg. Chem.*, 1964, **3**, 1323.
19 D. A. Dows, A. Haim and W. K. Wilmarth, *J. Inorg. Nucl. Chem.*, 1961, **21**, 33.
20 (*a*) C. J. Timpson, C. A. Bignozzi, B. P. Sullivan, E. M. Kober and T. J. Meyer, *J. Phys. Chem.*, 1996, **100**, 2915; (*b*) P. Belser, A. von Zelewsky, A. Juris, F. Barigelletti and V. Balzani, *Gazz. Chim. Acta*, 1985, **115**, 723.
21 (*a*) H. E. Toma and M. S. Takasugi, *J. Sol. Chem.*, 1983, **12**, 547; (*b*) U. Mayer, *Pure Appl. Chem.*, 1979, **51**, 1697; (*c*) V. Gutmann, *Pure Appl. Chem.*, 1979, **51**, 2197.
22 H. E. Toma, C. J. Cunha and C. Cipriano, *Inorg. Chim. Acta*, 1988, **154**, 63.
23 D. T. Sawyer and J. L. Roberts, Jr., *Experimental Electrochemistry for Chemists*, Wiley, New York, 1974.
24 M. G. Kinnaird and D. G. Whitten, *Chem. Phys. Lett.*, 1982, **88**, 275.
25 K. Kalyanasundaram, in *Polypyridine and Porphyrin Complexes*, Academic Press, London, 1992.
26 Th. Foster, *Discuss. Faraday Soc.*, 1959, **27**, 7.
27 (*a*) J. F. Ojo, Y. Hasegawa, Y. Sasaki, K. Kunimasa, M. Abe and N. Ohta, *Inorg. Chem. React.*, 2000, **2**, 301; (*b*) Y. Sasaki, K. Umakoshi, A. Kikuchi and A. Kishimoto, *Pure Appl. Chem.*, 1997, **69**, 205.
28 M. H. Wall, Jr., S. Akimoto, T. Yamazaki, N. Ohta, I. Yamazaki, T. Sakuma and H. Kido, *Bull. Chem. Soc. Jpn.*, 1999, **72**, 1475.